Risperidone/cyclodextrin inclusion complex electrospun nanofibers for fast-disintegrating antipsychotic drug delivery

Tony Tan [a,1], Asli Celebioglu [b,1], Mahmoud Aboelkheir [b], Tamer Uyar [b,*]

[a] *Biological Sciences, College of Agriculture and Life Sciences, Cornell University, Ithaca, NY, 14853, USA*
[b] *Fiber Science Program, Department of Human Centered Design, College of Human Ecology, Cornell University, Ithaca, NY, 14853, USA*

A B S T R A C T

In this paper, the inclusion complexes (ICs) of hydroxypropyl-beta-cyclodextrin (HPβCD) and risperidone were electrospun into nanofibrous film for potential fast-disintegrating drug delivery system. Risperidone is used to treat bipolar disorder, schizophrenia, and mood swings from autism. However, it is practically insoluble in aqueous medium. On the other hand, the encapsulation of risperidone into HPβCD cavity by inclusion complexation can enhance water solubility of this drug molecule. Here, the IC systems were prepared with 4/1 and 2/1 M ratio (HPβCD/risperidone). The highly concentrated HPβCD aqueous solutions (200 %, w/v) were used for the fiber formation. Finally, the system having 4/1 M ratio resulted in a clear and homogeneous solution showing that the HPβCD and risperidone completely formed IC. However, HPβCD/risperidone-IC having 2/1 M ratio was turbid and contained some small clumps of un-complexed risperidone. Even so, free-standing and thin nanofibrous films were obtained for both systems with an average fiber diameter of ~315 nm and ~280 nm for 2/1 and 4/1 systems, respectively. Both HPβCD/risperidone-IC nanofibers were produced with approximately 100 % preservation of risperidone within the nanofiber matrix without the loss of risperidone during electro-spinning process, that is, HPβCD/risperidone-IC nanofibers retained the initial M ratio of 2/1 and 4/1 as in electrospinning solution. Both HPβCD/risperidone-IC nanofibrous films showed fast-disintegration and fast-release characteristics in artificial saliva and aqueous medium verifying their potential as a fast-disintegrating oral drug delivery system for risperidone.

1. Introduction

Orally fast-disintegrating drug delivery systems have gained interest in the pharmaceutical manufacturing. The advantage they possess over traditional tablets is they rapidly dissolve or disintegrate in the oral cavity, without need of water [1]. This offers a convenient way of administering medications, to both people with swallowing difficulties and to the general population by enhancing bioavailability [1,2]. Electrospinning is a technique used to form nanofibers by the creation and elongation of an electrified fluid jet [3]. The highly porous, soft, light-weight, free-standing and flexible nature of electrospun nanofibers can be applied to drug delivery systems for a variety of substances ranging from antibiotics to proteins and DNA [4]. Here, the advantage of electrospinning also arises from providing a wide range of release profiles from fast to controlled ones for the variety of drugs that can be encapsulated by the fibers [5,6]. In addition to a basic single-fluid system [7], the properties of nanofibrous films can be diversified by applying a variety of electrospinning configurations including side-by-side [8], coaxial [8,9], and multiple-fluids [8,10]. These acquirements can also go ahead by incorporating nanofibers with additional encapsulation agents to attain effects including an improved bioavailability, solubility, stability, etc. Cyclodextrins are one of these agents among many others which have been used for the incorporation of different drug molecules into polymeric nanofibrous matrix [11–15].

Cyclodextrins (CDs) are a group of cyclic oligosaccharides composed of multiple glucose ring subunits joined by α-1,4 glycosidic bonds. These subunits form a toroidal shape ring, with a cone-shaped cavity [16,17]. This toroidal shape has a hydrophilic exterior that gives CD their water solubility, and a relatively more hydrophobic interior allows it to host hydrophobic molecules. When molecules of interest bind in the interior cavity of CDs by inclusion complexation, the water solubility, thermal stability, and bioavailability can be improved for a variety of compounds

[16,17]. Especially, an increased solubility of drug molecules can improve the drug's effectiveness at lower doses, decreasing the required administration amount, leading to a reduction in drug toxicity [18].

Risperidone is a second-generation atypical antipsychotic for the treatment of schizophrenia, bipolar disorder and autism irritability [19]. For the release of risperidone, various type of substrates such as nanoparticles, microparticles or implants were developed using different type of polymers including poly (D,L-lactide-co-glycolide) (PLGA), Eudragit S100, hydroxypropylmethyl cellulose (HPMC), polycaprolactones (PCL) and chitosan [20–24]. On the hand, risperidone is categorized by the biopharmaceutical classification system (BCS) as a class II drug because of its insolubility in water. As a class II drug, the absorption from the gastrointestinal tract and bioavailability is mainly limited by its dissolution rate [25]. It has been shown the solubility and so the bioavailability of risperidone can be improved by forming inclusion complexes with different types of CD derivatives for different treatment purposes [26–30]. Compared to natural CD, the derivative CD of hydroxypropyl-beta-cyclodextrin (HPβCD) shows higher water solubility which enables it to produce free-standing nanofibers by using its highly concentrated aqueous solutions [31]. Therefore, HPβCD was chosen for the generation of polymer-free nanofibers from the inclusion complexes of risperidone in this study. It is also noteworthy to mention that HPβCD has been proved to be well tolerated by animals and humans with its limited toxicity principally when it is taken orally [32]. Since previous studies have shown an enhanced solubility for different drug molecules which were complexed with HPβCD in the form of nanofibrous films [33–37], HPβCD/risperidone inclusion complex nanofibers have been produced for the development of an orally fast-disintegrating delivery system to act as an alternative to the traditional risperidone tablets and injections (Fig. 1). This approach also offers an alternative to the polymeric nanofibrous system developed for a fast-disintegrating delivery system in which different organic solvents or their blends are dominantly being used [38–40], unlike this recent study in which water was used as the solvent. The structural characteristics and pharmacotechnical properties of nanofibrous films were investigated using further techniques. Within our knowledge, polymer-free nanofibrous films of risperidone inclusion complexes with HPβCD or any other CD or CD derivatives have not been reported in the literature yet, that can be an alternative drug delivery approach for the risperidone.

## 2. Materials and methods

2.1. Materials

Hydroxypropyl-beta-cyclodextrin (HPβCD, Cavasol W7, DS: ~0.9) was donated by Wacker Chemie AG (USA). Risperidone (99 %, Fisher Scientific), methanol (≥99.8 % (GC), Sigma-Aldrich), phosphate buffered saline tablet (Sigma Aldrich), o-phosphoric acid (85 %, HPLC, Fisher Chemical), sodium chloride (NaCl, >99 %, Sigma Aldrich), sodium phosphate dibasic heptahydrate (Na_2HPO_4, 98.0–102.0 %, Fisher Chemical), potassium phosphate monobasic (KH_2PO_4 ≥99.0 %, Fisher Chemical), and deuterated dimethyl sulfoxide (DMSO-d_6, 99.8 %, Cambridge Isotope) were obtained commercially. Millipore Milli-Q ultrapure system (Millipore, USA) was used for water.

2.2. Phase solubility

To determine risperidone's phase solubility profile, a constant amount of risperidone powder exceeding its solubility (~0.12 mM) was mixed with 5 mL of water and HPβCD in increasing concentrations (0–12 mM). The samples were positioned on an orbital shaker in the dark for 24 h at 450 rpm at room temperature shielded from light. After 24 h, a 0.45 μm PTFE filter was used to filter the undissolved drug in each solution. The absorbance curves of filtered solutions were obtained using UV–vis spectroscopy (Perkin Elmer, Lambda 35, USA) (236 nm). The absorption results were adapted to concentration (mM) using a calibration curve of risperidone dissolved in a 1:1 (v:v) methanol-water solution which showed linearity with $R^2 \geq 0.99$. The following equation was applied to calculate the binding constant.

$$K_s = slope/S_0(1\text{-}slope) \tag{Eq. 1}$$

K_s is the binding constant and S_0 is the intrinsic solubility of risperidone powder (~0.12 mM) with no HPβCD present [41]. The phase solubility tests were done in triplicates and the results were given as an average ± standard deviation. Here, it is noteworthy to mention that, there was no detected effect of HPβCD existence on the UV absorbance profile of risperidone that can disturb the calculation.
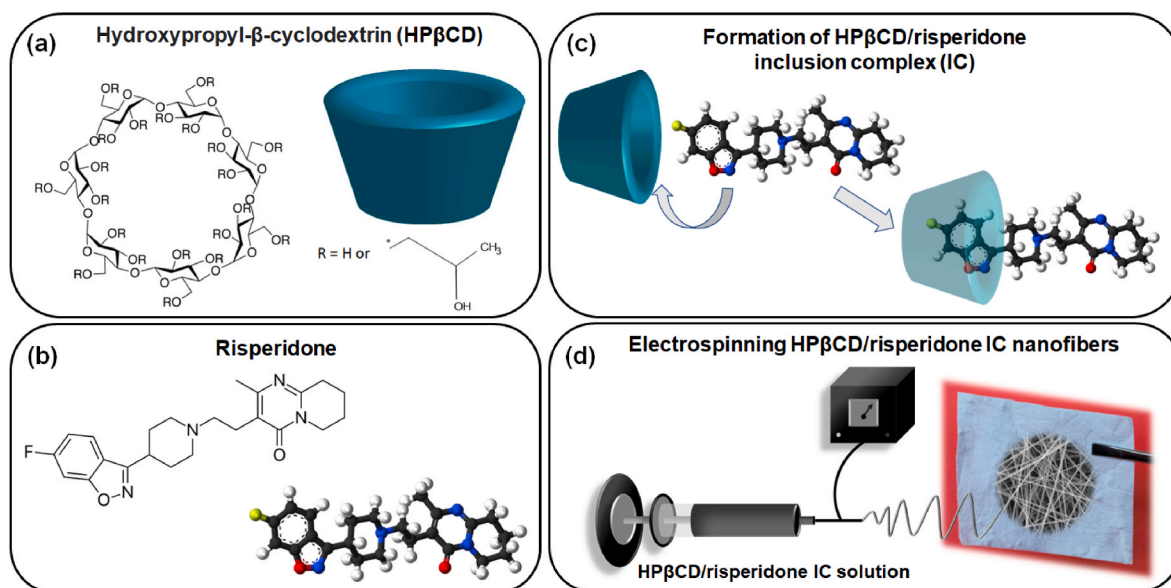
Fig. 1. The concept of study. (a) Chemical structure and schematic illustration of HPβCD and (b) risperidone. (c) Schematic representation of the formation of the HPβCD/risperidone inclusion complex (IC) and (d) the electrospinning of HPβCD/risperidone IC nanofibers.

2.3. 2D-NMR Measurement

The Rotating frame Overhauser Effect Spectroscopy (ROESY) experiment was performed for the inclusion complexes of HPβCD and risperidone using 600 MHz Varian INOVA nuclear magnetic resonance spectrometer in D_2O:DMSO-d_6 (3:1, v:v) system at 25 °C.

2.4. Preparation of electrospinning systems

200 % (w/v) concentrated HPβCD solutions were prepared in distilled water for both pristine HPβCD and inclusion complex (IC) systems. For IC systems, risperidone powder was added to the clear HPβCD solutions to create a separate 4/1 and 2/1 M ratio of HPβCD/ risperidone and they were stirred at 50 °C overnight to form inclusion complexes. Here, the M ratio of 4/1 and 2/1 corresponded to 6.8 % and 12.7 % (w/w, with respect to total sample amount) of risperidone content, respectively. The solution properties; viscosity and conductivity are major factors to the electrospinning process and nanofiber morphology. Therefore, prior to electrospinning, the conductivity of pure HPβCD, 2/1 and 4/1 HPβCD/risperidone-IC solutions were measured with a conductivity meter (Mettler Toledo FiveEasy) at room temperature. The viscosity of the same samples was measured by a rheometer (AR 2000 rheometer, TA Instrument, USA) configured with a 20 mm cone plate with a shear range of $0.01–1000$ s^{-1} at 21 °C.

The electrospinning was conducted via electrospinning equipment (Spingenix, model: SG100, Palo Alto, USA). For this, HPβCD and HPβCD/risperidone-IC solutions were drawn into separate 1 mL syringes fixed with 23G or 27G needles. A syringe pump was used to push out the solutions at a flow rate of 0.5 mL/h for all three samples. A positive charge was applied to the needle with a high voltage power supply at 17.5 kV. The solutions were electrospun at ~20 °C and in the range of 40–70 % relative humidity. Under these conditions, nanofibers were collected on a sheet of aluminium foil on a grounded plate approximately 15 cm from the needle.

2.5. Physicochemical characterization

The scanning electron microscope (SEM, Tescan MIRA3, Czech Republic) images of HPβCD/risperidone-IC and pristine HPβCD nanofibers were obtained to analyze fiber morphology. To reduce charging during SEM imaging, a thin Au/Pd layer was coated on the samples. The average fiber diameter (AFD) of ~100 nanofibers per sample were calculated using the SEM images and ImageJ software and were given as mean values ± standard deviations. The complexation status of samples was verified with attenuated total reflectance Fourier transform infrared (ATR-FTIR) spectrometer (PerkinElmer, USA). The FTIR spectra of risperidone powder, HPβCD nanofiber, and HPβCD/risperidone-IC nanofibers were obtained with 32 scans from a wavenumber range of 4000 cm^{-1} to 600 cm^{-1}, with a resolution of 4 cm^{-1}. To obtain data on the thermal properties of samples, a thermogravimetric analyzer (TGA, Q500, TA Instruments, USA) and differential scanning calorimeter (DSC, Q2000, TA Instruments, USA) were used. For TGA, the samples were loaded onto a platinum pan and heated at a rate of 20.0 °C per minute starting at room temperature and ending at 550 °C under N_2. For DSC, Tzero aluminium pans were used to be loaded with the samples and heated at a rate of 10.0 °C per minute starting at 0 °C and ending at 250 °C under N_2. X-ray diffractometry (XRD, Bruker D8 Advance ECO) was utilized to observe the diffraction pattern of risperidone powder, HPβCD nanofibers, and HPβCD/risperidone-IC nanofibers. All samples were examined at the 2θ between 5° and 30° with the voltage set to 40 kV and current at 25 mA (radiation source: Cu Kα). Proton nuclear magnetic resonance (^{1}H NMR) spectra were recorded using a Bruker AV500 nuclear magnetic resonance spectrometer having an autosampler at 25 °C. For this, risperidone powder was dissolved in DMSO-d_6 at ~8 g/L, and HPβCD nanofibers and HPβCD/risperidone-IC nanofibers were dissolved in DMSO-d_6 at 60 g/L sample concentration, and all samples

were scanned 16 times. The software Mestrenova was used to integrate the chemical shifts (δ, ppm) of each sample. The peaks of HPβCD (-CH$_3$; 1.03 ppm) and risperidone (aromatic protons; 7.25–8.04 ppm) were used to calculate the M ratio of HPβCD/risperidone in HPβCD/risperidone-IC (2/1 and 4/1) nanofibers.

2.6. Pharmacotechnical profiles

To determine the release of risperidone from the HPβCD/risperidone-IC nanofibrous films over time, ~10 mg samples in 10 mL of PBS buffer solution (pH 7.4) were shaken on an orbital shaker for 10 min at 37 °C and at 200 rpm. Aliquots of 0.5 mL were taken at predetermined time intervals and 0.5 mL of fresh PBS was added to these aqueous systems. The absorbance values of the aliquots were obtained using UV–vis spectroscopy (236 nm). For each sample, the measurements were performed in triplicates and the absorbance results were converted to released percent over time. To study the disintegration profile, artificial saliva, composed of 2.38 g Na_2HPO_4, 0.190 g KH_2PO_4 and 8 g NaCl in 1L distilled water, with phosphoric acid to adjust the pH to 6.8 was used [42]. Two similar sized samples of 2/1 and 4/1 HPβCD/risperidone-IC nanofibrous films (~3.5 × 5.5 cm) were placed onto 2 separate 10 cm Petri dishes, each with a filter paper soaked with 10 mL of artificial saliva, with the excess artificial saliva removed to mimic the oral cavity. A recording (Video S1) was obtained using a mobile device for the disintegration time of the samples.

2.7. Statistical analysis

The repeated experiments' result were specified as mean values ± standard deviations. The statistical analysis was performed using one-way or two-way of variance (ANOVA, OriginLab (Origin 2023, USA)) (0.05 level of probability).

3. Results and discussion

3.1. Phase solubility analysis

The phase solubility analysis was conducted for upward concentration of HPβCD to observe its effect on risperidone solubility, and Fig. 2 shows the phase solubility graph of risperidone with an HPβCD concentration of 0–12 mM. The intrinsic solubility of risperidone was determined to be approximately 0.12 mM. Due to the presence of
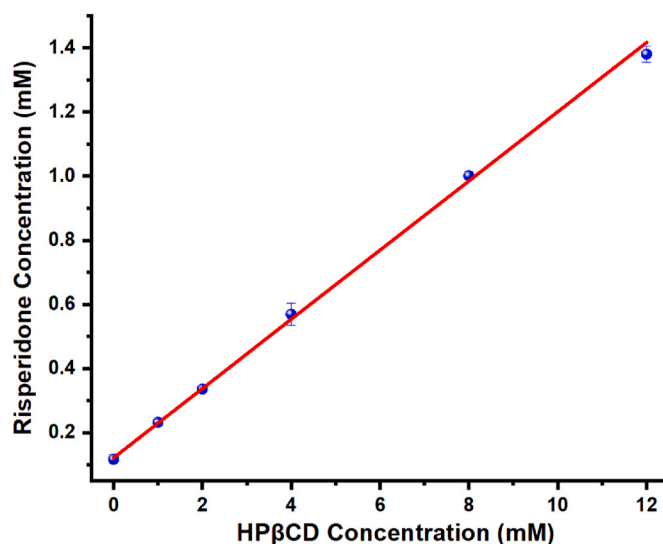

Fig. 2. Phase solubility profile. Phase solubility diagram of the HPβCD/risperidone inclusion complex system.

HPβCD, risperidone solubility was increased by ~11.7 times in the 12 mM HPβCD solution. Statistical analysis revealed varying HPβCD concentrations had a statistically significant difference on the samples, resulting in $p \ll 0.05$. Phase solubility diagrams can follow different trends, and here an A_L-type pattern, which is obtained when the guest solubility increases linearly with the increasing host concentration was detected for risperidone and HPβCD for the given conditions [41]. The K_s value calculated from the linear part of phase solubility diagram, indicates the binding strength between guest molecules and CD cavity, where a higher value corresponds to a strong binding. In this study, the K_s value was calculated to be 1007 M^{-1} for the HPβCD/risperidone system which revealed the strong binding and favorable inclusion complexation between these two components. This is coherent with the previous study in which the K_s values were found to be 1308.33 M^{-1} in case of using HPβCD [28].

3.2. 2D-NMR (ROESY) analysis

Nuclear Overhauser Effect Spectroscopy (NOESY) and Rotating Frame Overhauser Effect Spectroscopy (ROESY) are prominent two-
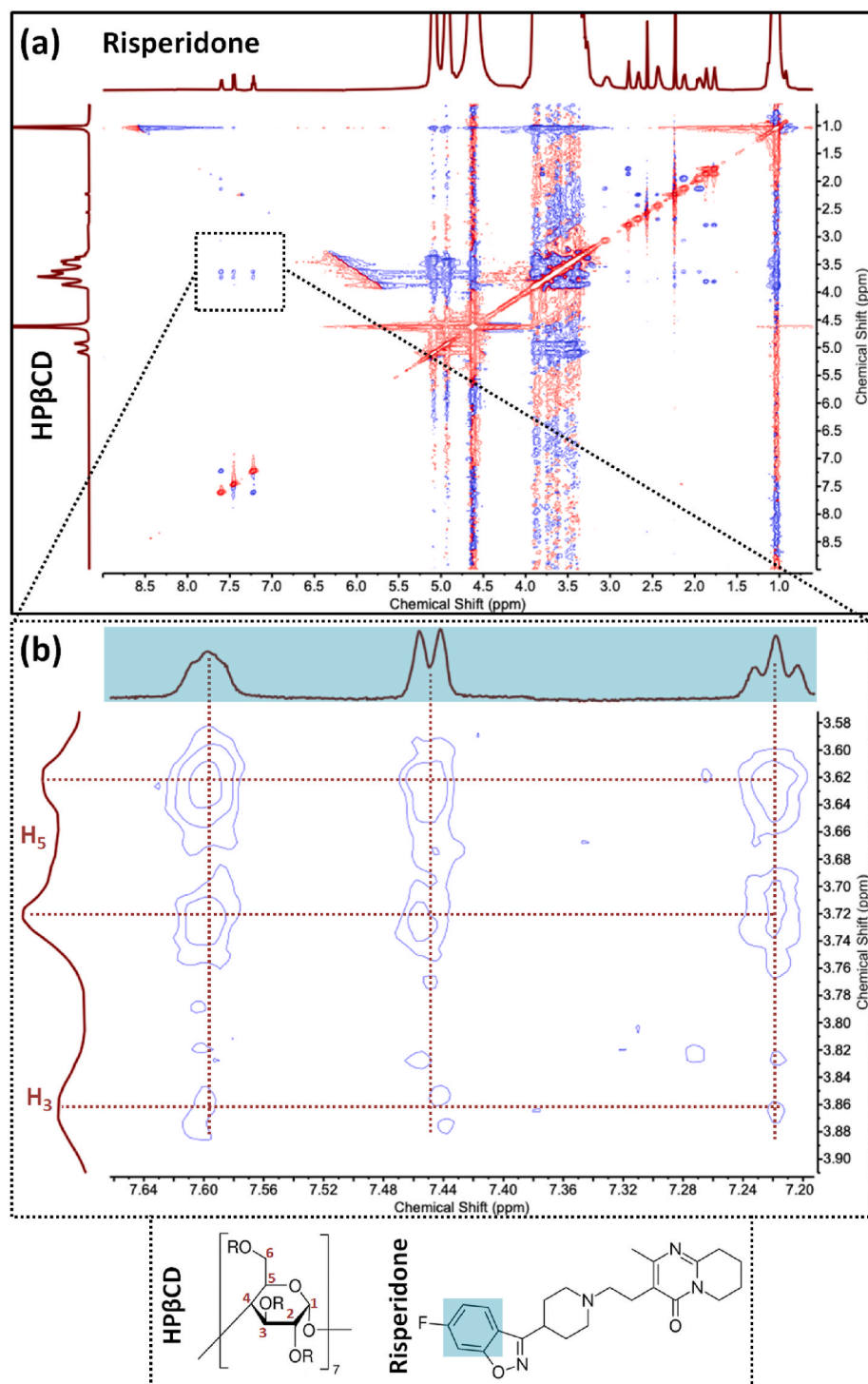

Fig. 3. The chemical characterization. (a) Full and (b) expanded 2D-NMR (ROESY) spectra of risperidone and HPβCD recorded in D$_2$O:DMSO-d_6 (3:1, v:v).

dimensional Nuclear Magnetic Resonance (2D-NMR) techniques widely employed for investigating interactions involving CDs with a diverse range of guest molecules, spanning organic, inorganic, and hybrid compounds. Notably, ROESY, with its exceptional capability to probe interactions over extended distances, up to 5 Å, is preferred over NOESY, especially for examining nanoscale assemblies constructed with CDs [43,44]. In this study, ROESY NMR technique was utilized to elucidate spatial host-guest interactions in a solution containing HPβCD and risperidone. Analysis of the ROESY spectra for the HPβCD/risperidone system revealed simultaneous proton resonances between the inner cavity protons (H_3 and H_5) of HPβCD and the aromatic protons on the fluorinated ring of risperidone (Fig. 3). This observation unequivocally indicated the formation of inclusion complexes between HPβCD and risperidone, and also highlighted the efficacy of ROESY in capturing the essence of these host-guest interactions.
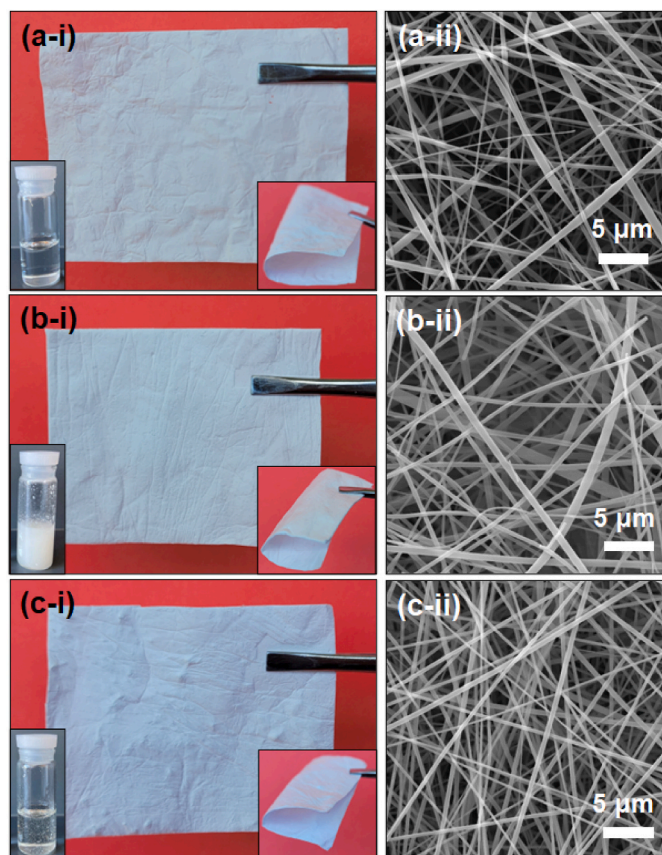
3.3. Physicochemical characteristics of samples

Here, a clear aqueous solution of pristine HPβCD was obtained using 200 % (w/v) of solid concentration (Fig. 4a–i). On the other hand, it is known from the previous reports, risperidone can form inclusion complexes with HPβCD efficiently by 2/1 (CD/drug) M ratio [27,30]. Therefore, the inclusion complex nanofibers were first prepared using 2/1 (HPβCD/risperidone) M ratio. However, it was observed that the HPβCD/risperidone-IC (2/1) solution was turbid, with clumps of undissolved risperidone distributed throughout the solution (Fig. 4b–i). Here, the reason for the heterogeneous state of the 2/1 system might be the high concentration of HPβCD solution and so its high viscosity which

Fig. 4. The visual and morphological analysis. Photos of electrospun nanofibers, the solution used for their electrospinning, the SEM images of the nanofibers, and the diameter distribution. (a) HPβCD nanofibers, (b) HPβCD/risperidone-IC (2/1) nanofibers, and (c) HPβCD/risperidone-IC (4/1) nanofibers.

might have inhibited the efficient stirring of the system to obtain complete complexation between risperidone and HPβCD. In contrast, HPβCD/risperidone-IC (4/1) solutions prepared using less amount of drug resulted in clear and homogeneous solution just like pristine HPβCD solution (Fig. 4c–i). This suggested that a complete complexation occurred for HPβCD/risperidone-IC (4/1) system where all risperidone formed an inclusion complex with HPβCD. Here, all solutions provided free-standing and flexible nanofibrous films, perfectly suited for drug delivery purposes, as depicted in Fig. 4 a,b,c-i. These nanofiber networks were also able to be folded without damage (Fig. 4 a,b,c-i). Fig. 4 a,b,c-ii show the SEM images of the pristine HPβCD, HPβCD/risperidone-IC (2/1) and HPβCD/risperidone-IC (4/1) nanofibers, respectively. All three solutions were able to generate nanofibers having defect-free and homogenous morphology (Fig. 4 a,b,c-ii).

The solutions' viscosity, conductivity, and average fiber diameters (AFD) for pristine HPβCD, HPβCD/risperidone-IC (2/1) and HPβCD/risperidone-IC (4/1) nanofibers were summarized in Table 1. Here, the AFD differences can be attributed to the variation between solution properties including conductivity and viscosity. Principally, higher conductivity results in greater self-repulsion of the electrospinning solution and this repulsion stretches the solution and creates thinner fibers [31,45]. On the other hand, lower viscosity also allows for more and easier stretching of the solution that creates thinner fibers. As seen in Table 1, as the risperidone concentration increased, the viscosity of the solution increased, as well as the conductivity values decreased. As expected, pristine HPβCD solution containing no risperidone and having the highest conductivity and the lowest viscosity resulted in thinner fibers (240 ± 110 nm) than any of the other two inclusion complex samples (Table 1). On the other hand, HPβCD/risperidone-IC (2/1) solution containing the highest concentration of risperidone showed the lowest conductivity and highest viscosity among other solutions. As such, less stretching happened during the process and resulted into thicker fiber formation (315 ± 145 nm) compared to pristine HPβCD and HPβCD/risperidone-IC (2/1) systems. The observed AFD of HPβCD/risperidone-IC (4/1) nanofibers were found in between that of pristine HPβCD and HPβCD/risperidone-IC (2/1) with 280 ± 75 nm of AFD. The statistical analysis revealed the means values of nanofibers are significantly different from each other's ($p \ll 0.05$)).

The FTIR was used both to verify the presence of risperidone in the HPβCD/risperidone-IC nanofibers and the inclusion phenomenon within the samples. Depending on the interaction between CD and guest molecules, attenuations, shifts, or disappearances of characteristic peaks can be observed in the FTIR spectra [46]. The FTIR spectra of risperidone, HPβCD, and HPβCD/risperidone-IC nanofibers were depicted in Fig. 5. For all nanofibrous film-based samples, there was a broad peak existing in 3000–3600 cm^{-1} and it is due to the –OH groups of HPβCD [47]. Between the 1020 and 1150 cm^{-1} region, a strong peak was observed, and this is the result of the coupled C–C/C–O stretching and antisymmetric C–O–C glycosidic bridge stretching [47]. These distinguished peaks and the majority of the FTIR scan confirmed the huge content of

Table 1
The solution properties and the fiber diameters of the resulting electrospun nanofibers.

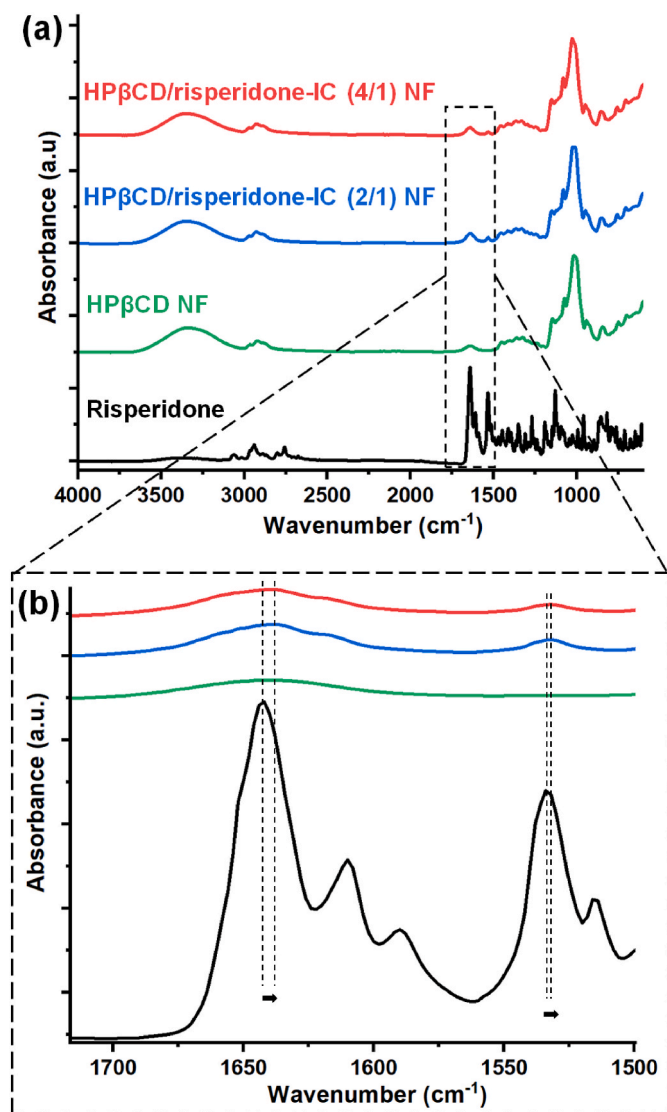| Sample	Risperidone conc. (w/w)*	Viscosity (Pa·s)	Conductivity (μS/cm)	Average fiber diameter (nm)
HPβCD	–	1.037	36.61	240 ± 110
HPβCD/ risperidone (4/1)	6.8 %	1.870	30.65	280 ± 75
HPβCD/ risperidone (2/1)	12.7 %	2.181	29.85	315 ± 145

*With respect to total sample amount.

Fig. 5. The chemical characterization. (a) The full and (b) expanded FTIR spectra of risperidone powder, pristine HPβCD nanofibers, and HPβCD/risperidone-IC (2/1 and 4/1) nanofibers.

Fig. 6. The crystallinity analysis. (a) DSC thermograms and (b) XRD graphs of risperidone powder, pristine HPβCD nanofibers, and HPβCD/risperidone-IC (2/1 and 4/1) nanofibers.

HPβCD (~87–93 %, w/w) in both inclusion complex nanofibers (Fig. 5a). However, the expanded FTIR spectrum (1750-1500 cm^{-1}) given in Fig. 5b, depicted the existence of characteristic peaks of risperidone in HPβCD/risperidone-IC (2/1) and HPβCD/risperidone-IC (4/1) nanofibers. Here, the distinct peak at 1642 cm^{-1} is due to C=O stretching from tetrahydropyrido-pyrimidinone ring, and the other distinct peak at 1534 cm^{-1} corresponds to C=C stretching of the aromatic ring of risperidone [48–50]. Other peaks of risperidone peaks were masked by the characteristic peaks of HPβCD. The FTIR finding showed that the peak at 1642 cm^{-1} shifted to 1638 cm^{-1} and the peak at 1534 cm^{-1} shifted to 1532 cm^{-1} for both inclusion complex nanofibers (Fig. 5b). Both of these shifts revealed that the risperidone molecules were encapsulated into HPβCD by inclusion complexation from the ends of the risperidone structure which is composed of aromatic and pyrimidinone rings.

The DSC measurement was performed to examine the difference between pristine HPβCD and HPβCD/risperidone-IC nanofibers from the point of the melting point of the drug that shows the crystallinity of the risperidone. Here, the inclusion complexation can lead to decrease, disappearance or shift at the melting point of guest molecules [51]. In Fig. 6a, a broad endothermic peak can be observed between 50 °C and
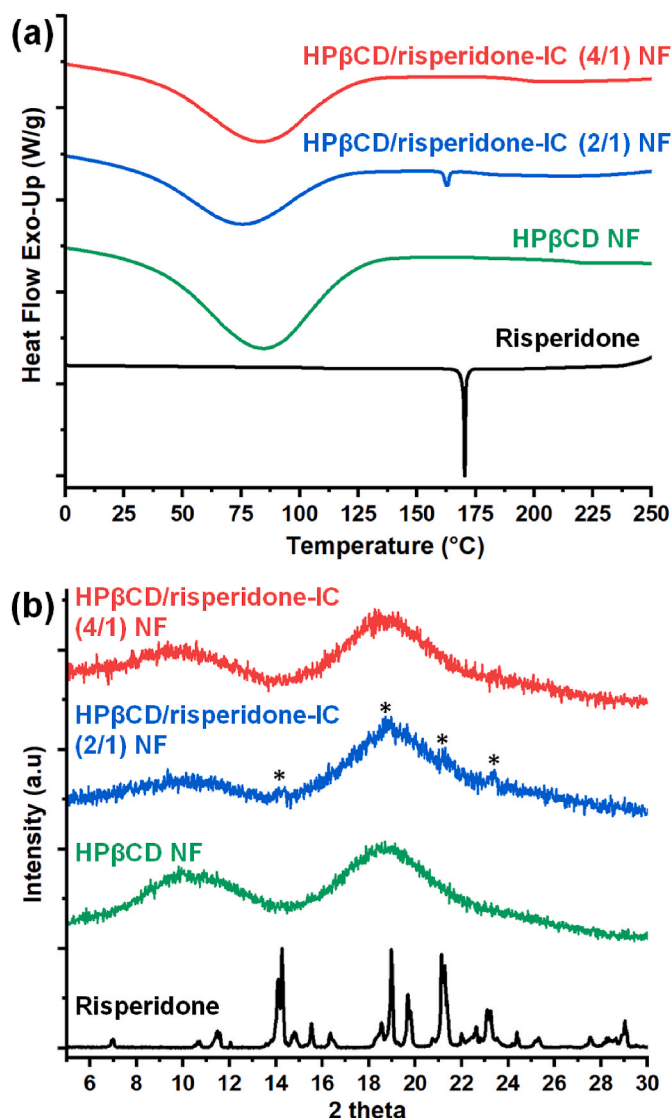
100 °C for all nanofibrous film samples corresponding to the evaporation of water. The risperidone powder showed a sharp peak at 170 °C, which corresponds to the melting point highlighting the crystal structure. For HPβCD/risperidone-IC (2/1) nanofibers, the peak at around 162 °C with a lower intensity showed that some part of risperidone in this sample could not form inclusion complex and kept into the crystal structure. On the other hand, the DSC thermogram of HPβCD/risperidone-IC (4/1) nanofibers closely resembled that of the pristine HPβCD nanofibers. The absence of the melting point of risperidone showed that all risperidone incorporated into HPβCD/risperidone-IC (4/1) nanofibers has efficiently formed an inclusion complex.

The XRD technique was also used to analyze the crystalline patterns of the samples to confirm the amorphization of risperidone crystals by inclusion complexation. The XRD patterns of risperidone powder, HPβCD nanofibers and HPβCD/risperidone-IC (2/1 and 4/1) nanofibers were shown in Fig. 6b. The diffraction pattern of risperidone powder shows four prominent sharp peaks at 2θ = 14.2°, 18.9°, 21.1°, 23.1°. On the other hand, HPβCD nanofibers indicated two broad halos at 10.9° and 18.7° due to its amorphous nature. HPβCD/risperidone-IC (4/1) nanofibers had diffraction pattern that closely followed that of HPβCD nanofibers, and no characteristic risperidone diffraction peaks were

observed (Fig. 6b). Thus, it is reasonable to conclude risperidone crystals were not present and the formation of an inclusion complex with HPβCD prevented crystals from forming. Conversely, the XRD graph of HPβCD/risperidone-IC (2/1) nanofibers indicated the characteristic peaks of risperidone at the same 2θ ranges with lower intensity. This result also showed that some part of risperidone could not form an inclusion complex and remained in crystal form in case of HPβCD/risperidone-IC (2/1) nanofibers. Here, both DSC and XRD findings were correlated with the visual observation of the HPβCD/risperidone-IC (2/1) solution, which was turbid and not clear like HPβCD/risperidone-IC (4/1) solution (Fig. 4). This result was critical to be observed that the drugs in the amorphous state can enable the fast-dissolution and fast-release systems.

The thermal degradation profile of samples was further analyzed through TGA, and the results were shown in Fig. 7. Risperidone indicated one step mass loss from 250 °C to 510 °C, which was consistent with previous risperidone thermal degradation measurement. Pristine HPβCD nanofibers showed two regions of weight loss. The first step observed between 0 °C and 100 °C corresponds to the evaporation of water. The second major weight loss was between 300 °C and 400 °C, and this was due to thermal degradation of HPβCD. In both HPβCD/risperidone-IC (2/1) and HPβCD/risperidone-IC (4/1) nanofibers, the degradation patterns closely resembled that of HPβCD nanofibers with a slight difference at the main degradation peak. In the derivative

thermograms (DTG) shown in Fig. 7b, there was a reduction in the peak intensity of HPβCD in case of HPβCD/risperidone-IC nanofibers depending on the risperidone content. Additionally, the main degradation of HPβCD nanofibers starting at 295 °C shifted to a lower temperature of 280 °C and 285 °C for HPβCD/risperidone-IC (2/1) and HPβCD/risperidone-IC (4/1) nanofibers, respectively. This was a result of risperidone's lower starting degradation temperature loaded in the electrospun nanofibrous films. The thermal degradation peaks in Fig. 7b highlighted that they were shifted from 357 °C for HPβCD nanofibers to 354 °C and 360 °C for HPβCD/risperidone-IC (2/1) and HPβCD/risperidone-IC (4/1) nanofibers, respectively. The main peak of HPβCD/risperidone-IC (2/1) shifted to the lower value can be attributed to the uncomplexed risperidone content in the nanofibers. There was even a shoulder detected at around 286 °C which was another indication of crystal and uncomplexed risperidone existence. However, the main peak HPβCD/risperidone-IC (4/1) nanofibers shifted to the higher temperature range compared to pristine HPβCD and this can be due to complete complex formation between HPβCD and risperidone molecules.

Prior to electrospinning process, the M ratio of the HPβCD/risperidone-IC solutions were set as 2/1 and 4/1 (CD/drug), however, due to the efficiency of the complexation and electrospinning processes, the M ratio after electrospinning may deviate from the initial ratio. Using ^{1}H NMR, the M ratios of the ultimate inclusion complex nanofibers were determined through integrating the peak of the methyl group of HPβCD (1.03 ppm) and the peak of the aromatic protons (7.25–8.04 ppm) in risperidone (Fig. 8) [52]. Although HPβCD/risperidone-IC (2/1) nanofibers were proven to have uncomplexed risperidone, this did not affect the calculations due to risperidone being highly soluble in DMSO-d_6, the NMR solvent. The NMR results proved that both HPβCD/risperidone-IC nanofibers were obtained with the initial M ratio of 2/1 and 4/1 (CD/drug) that correspond to 12.7 % and 6.8 % (w/w) of risperidone content, respectively. In other words, the electrospinning process was performed efficiently without loss of drug. Here, the nanofibrous films of CD/risperidone inclusion complexes could be obtained with the drug loading capacity of ~7–13 mg/100 mg (drug/nanofibrous film). Thus, risperidone daily doses that change between 0.25 mg and 6 mg for different diseases and ages [53] can be met by using the required amount of nanofibrous film (mg). It is also noteworthy to mention that the characteristic peaks of risperidone with the same pattern were observed for the inclusion complex nanofibers. This confirmed the preserved chemical structure of the drug throughout all these processes.

3.4. Pharmacotechnical profiles of nanofibrous films

Fig. 9a shows the time-dependent *in-vitro* release profile of HPβCD/risperidone-IC nanofibers in PBS buffer (pH 7.4). HPβCD/risperidone-IC (2/1) and HPβCD/risperidone-IC (4/1) nanofibers released 76.4 ± 8.4 % and 90 ± 12.1 % of risperidone in the first 30 s, respectively. Afterward, HPβCD/risperidone-IC (2/1) nanofibers indicated a slight increase up to 2 min, however, both inclusion complex nanofibrous films showed an almost plateau profile till the end of 10 min. Here, the relatively faster and higher release profile of HPβCD/risperidone-IC (4/1) nanofibers originated from the full complexation with risperidone and HPβCD. The small amount of uncomplexed risperidone might be the reason for the fairly worse performance of HPβCD/risperidone-IC (2/1) nanofibers. Even so, the high release percentages in the given time verifies HPβCD/risperidone-IC nanofibers had fast dissolving and release properties that raised from the enhanced solubility of risperidone by inclusion complexation, high water-solubility of HPβCD and high surface area/porous structure of the nanofibers. Statistical analysis shows nonsignificant variations between the release profile of HPβCD/risperidone-IC (4/1 and 2/1) nanofibers (p ≫ 0.05). Kinetic models were also used to further analyze the release profile of HPβCD/risperidone-IC (4/1 and 2/1) nanofibers. Table S1 summarized the R^2 (regression coefficient) values found by using different kinetic model calculation. The finding indicated that both HPβCD/risperidone-IC (2/1) nanofibers and HPβCD/
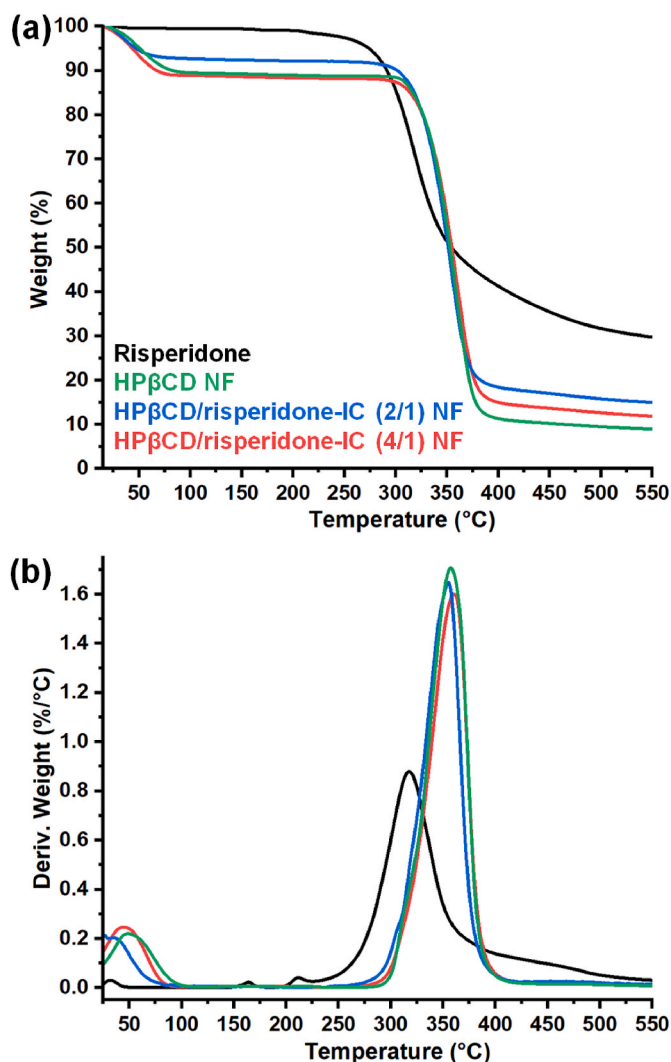

Fig. 7. Thermal characterization. (a) TGA thermograms and (b) derivatives thermograms (DTG) of risperidone powder, pristine HPβCD nanofibers, and HPβCD/risperidone-IC (2/1 and 4/1) nanofibers.

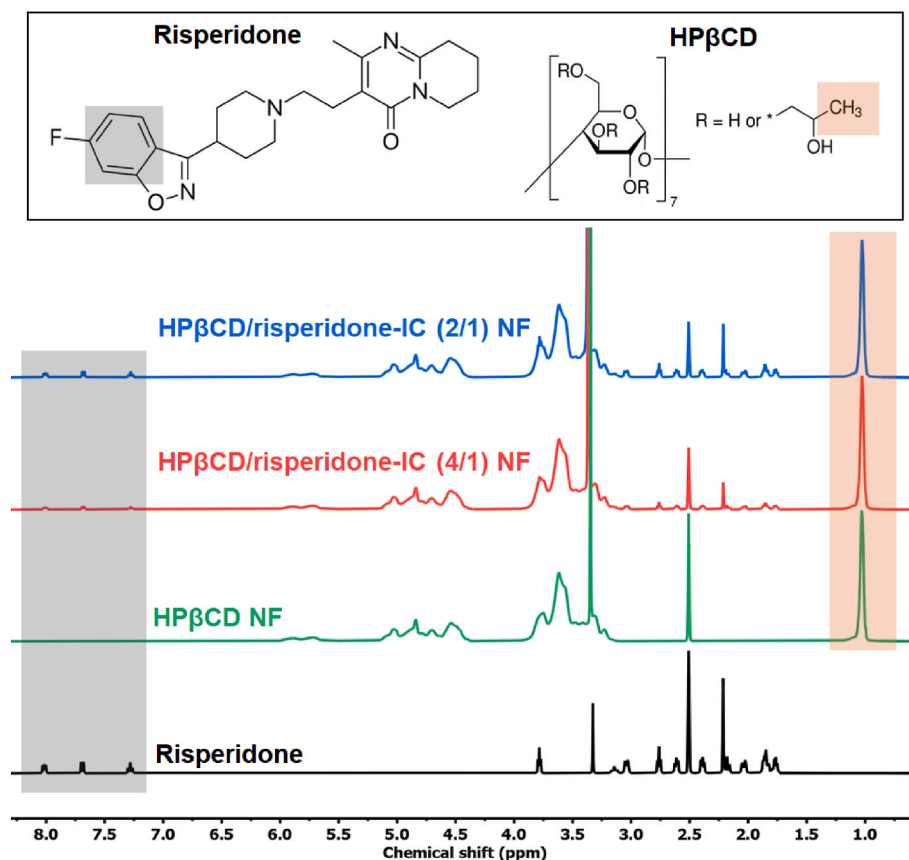**Fig. 8. The chemical characterization.** ^{1}H NMR of risperidone, pristine HPβCD nanofibers, and HPβCD/risperidone-IC (2/1 and 4/1) nanofibers.

risperidone-IC (4/1) nanofibers did not display compatibility with neither zero/first-order kinetics nor Higuchi models (Table S1). These results revealed that Fick's first law which shows the time-dependent release of drug molecules from insoluble matrix, did not rule the release profile of nanofibers [54]. On the other hand, both HPβCD/risperidone-IC nanofibers exhibited relatively better consistency with Korsmeyer-Peppas model compared to other models (Table S1). This stated the diffusion and erosion-dependent release of risperidone from electrospun nanofibrous films. The diffusion exponent (*n*) values calculated by Korsmeyer–Peppas equations were distinguished in the range of 0.45 < n < 0.89 confirming the irregular diffusion and non-Fickian release of risperidone in the liquid medium [54].

Artificial saliva and filter paper were used to simulate the oral cavity to further observe the disintegration profiles of HPβCD/risperidone-IC nanofibers. Photos captured from Video S1 were depicted in Fig. 9b. For HPβCD/risperidone-IC (2/1) and HPβCD/risperidone-IC (4/1) nanofibers, it took ~ 10 s to completely disintegrate in artificial saliva environment. Here, both inclusion complex nanofibrous films rapidly disintegrated upon contact with medium and that was again the key feature of the high water-solubility of HPβCD coupled with the high surface area and porous nature of the nanofibers. These features allowed the medium to quickly spread throughout the nanofiber networks and disintegrate them in artificial saliva. HPβCD/risperidone-IC nanofiber films having fast-release and fast-disintegration properties can make it a possible candidate for fast-disintegrating oral delivery systems of risperidone.

4. Conclusions

In this study, electrospun nanofibers solely made of inclusion complexes of risperidone and HPβCD were developed in a 2/1 and 4/1 HPβCD/risperidone-IC M ratio. The formation of the inclusion complexes was confirmed using ROESY (2D-NMR), DSC and XRD, and the presence of interactions between the risperidone molecules and HPβCD was furthers verified using TGA and FTIR. ^{1}H NMR data demonstrated that the electrospinning process was highly efficient, producing nanofibers with the same M ratio as the starting solution (~100 % of preservation). The inclusion complex nanofibrous films exhibited enhanced water solubility for risperidone, such that HPβCD/risperidone-IC (4/1) nanofibers released approximately 90 % of the risperidone within the first 30 s. Upon contact with a simulated oral cavity, both HPβCD/risperidone-IC (2/1) and HPβCD/risperidone-IC (4/1) nanofibrous films disintegrated within ~10 s. Additionally, phase solubility analysis demonstrated that the water solubility of risperidone can be enhanced by 11.7 times. It is noteworthy to mention that, the use of water as the sole solvent during the production of nanofibers, eliminated the need for potentially toxic or harmful chemicals, an advantage for large scale production of nanofibrous films of drug/cyclodextrin inclusion complexes. Overall, these results suggest that electrospun nanofibers have also potential in antipsychotic drug delivery systems. The nanofibrous films of HPβCD/risperidone-IC can offer a promising alternative for the administration of risperidone as an orally fast-disintegrating dosage formulation which can provide convenience for the patient during antipsychotic drug treatment.

CRediT authorship contribution statement

Tony Tan: Writing – original draft, Investigation. **Asli Celebioglu:** Writing – original draft, Methodology, Investigation, Formal analysis, Conceptualization. **Mahmoud Aboelkheir:** Investigation. **Tamer Uyar:** Writing – review & editing, Supervision, Resources, Project administration, Methodology, Funding acquisition, Conceptualization.
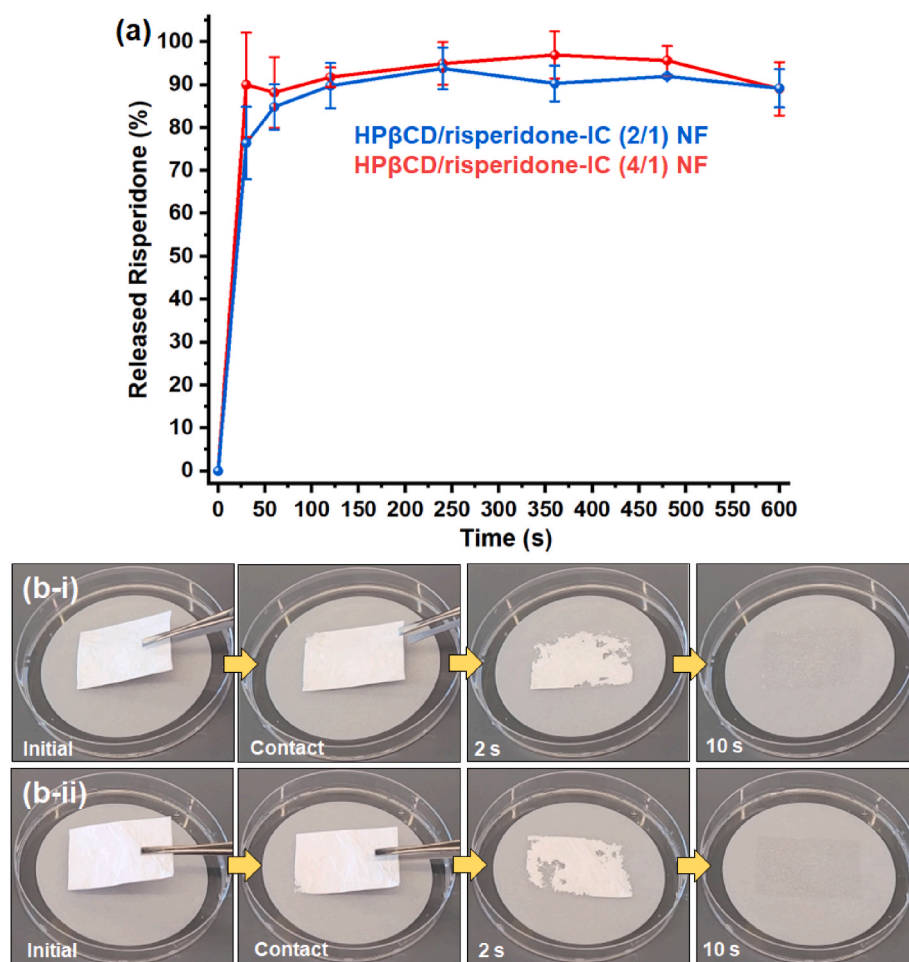
Fig. 9. Pharmacotechnical profiles. (a) Time dependent release profiles of HPβCD/risperidone-IC (2/1) and HPβCD/risperidone-IC (4/1) nanofibers. (b) The disintegration behavior of (i) HPβCD/risperidone-IC (2/1) and (ii) HPβCD/risperidone-IC (4/1) nanofibrous films in an artificial saliva environment. These photos were captured from the Video S1.

Declaration of competing interest

The authors declare that they have no known competing financial interests or personal relationships that could have appeared to influence the work reported in this paper.

Data availability

Data will be made available on request.

Appendix A. Supplementary data

Supplementary data to this article can be found online at https://doi.org/10.1016/j.jddst.2024.105753.

References

[1] F. Laffleur, V. Keckeis, Advances in drug delivery systems: work in progress still needed? Int. J. Pharm. 590 (2020) 119912.

[2] M. He, L. Zhu, N. Yang, H. Li, Q. Yang, Recent advances of oral film as platform for drug delivery, Int. J. Pharm. 604 (2021) 120759.

[3] A. Keirouz, Z. Wang, V.S. Reddy, Z.K. Nagy, P. Vass, M. Buzgo, S. Ramakrishna, N. Radacsi, The history of electrospinning: past, present, and future developments, Adv. Mater. Technol. 8 (2023) 2201723.

[4] Y. Si, S. Shi, J. Hu, Applications of electrospinning in human health: from detection, protection, regulation to reconstruction, Nano Today 48 (2023) 101723.

[5] A. Luraghi, F. Peri, L. Moroni, Electrospinning for drug delivery applications: a review, J. Contr. Release 334 (2021) 463–484.

[6] P. Ghasemiyeh, S. Mohammadi-Samani, A. Nokhodchi, An overview of nanofibers and microfibers for improved oral delivery of medicines: challenges and advances, J. Drug Deliv. Sci. Technol. (2023) 105235.

[7] S.M. Tan, X.Y. Teoh, J. Le Hwang, Z.P. Khong, R. Sejare, A.Q.A. Al Mashhadani, R. Abou Assi, S.Y. Chan, Electrospinning and its potential in fabricating pharmaceutical dosage form, J. Drug Deliv. Sci. Technol. (2022) 103761.

[8] J. Xing, M. Zhang, X. Liu, C. Wang, N. Xu, D. Xing, Multi-material electrospinning: from methods to biomedical applications, Mater. Today Bio. (2023) 100710.

[9] Y. Liu, X. Chen, X. Lin, J. Yan, D. Yu, P. Liu, H. Yang, Electrospun multi-chamber core–shell nanofibers and their controlled release behaviors: a review, Wiley Interdiscip. Rev. Nanomedicine Nanobiotechnology. 16 (2024) e1954.

[10] D. Yu, M. Wang, X. Li, X. Liu, L. Zhu, S.W. Annie Bligh, Multifluid electrospinning for the generation of complex nanostructures, Wiley Interdiscip. Rev. Nanomedicine Nanobiotechnology. 12 (2020) e1601.

[11] A. Dodero, G. Schlatter, A. Hébraud, S. Vicini, M. Castellano, Polymer-free cyclodextrin and natural polymer-cyclodextrin electrospun nanofibers: a comprehensive review on current applications and future perspectives, Carbohydr. Polym. (2021) 118042.

[12] A. Daghrery, Z. Aytac, N. Dubey, L. Mei, A. Schwendeman, M.C. Bottino, Electrospinning of dexamethasone/cyclodextrin inclusion complex polymer fibers for dental pulp therapy, Colloids Surf. B Biointerfaces 191 (2020) 111011.

[13] Z. Hussain, I. Ullah, Z. Wang, P. Ding, S. Ullah, Y. Zhang, Z. Zhang, J. Yan, B. Luo, R. Pei, Electrospun nanofibrous membrane functionalized with dual drug-cyclodextrin inclusion complexes for the potential treatment of otitis externa, Colloid. Surface. A Physicochem. Eng. Asp. 651 (2022) 129742.

[14] N. Sharifi, S.A. Mortazavi, S. Rabbani, M. Torshabi, R. Talimi, A. Haeri, Fast dissolving nanofibrous mats for diclofenac sodium delivery: effects of electrospinning polymer and addition of super-disintegrant, J. Drug Deliv. Sci. Technol. (2022) 103356.

[15] E. Hsiung, A. Celebioglu, M.E. Kilic, E. Durgun, T. Uyar, Fast-disintegrating nanofibrous web of pullulan/griseofulvin–cyclodextrin inclusion complexes, Mol. Pharm. 20 (2023) 2624–2633.

[16] G. Crini, A history of cyclodextrins, Chem. Rev. 114 (2014) 10940–10975.

[17] E.M.M. Del Valle, Cyclodextrins and their uses: a review, Process Biochem. 39 (2004) 1033–1046.

[18] S.S. Braga, Cyclodextrin superstructures for drug delivery, J. Drug Deliv. Sci. Technol. (2022) 103650.

[19] A.A. Bhat, G. Gupta, O. Afzal, I. Kazmi, F.A. Al-Abbasi, A.S.A. Altamimi, W. H. Almalki, S.I. Alzarea, S.K. Singh, K. Dua, Neuropharmacological effect of risperidone: from chemistry to medicine, Chem. Biol. Interact. (2022) 110296.

[20] M. Qureshi, M. Aqil, S.S. Imam, A. Ahad, Y. Sultana, Formulation and evaluation of neuroactive drug loaded chitosan nanoparticle for nose to brain delivery: in-vitro characterization and in-vivo behavior study, Curr. Drug Deliv. 16 (2019) 123–135.

[21] B. Yerragunta, S. Jogala, K.M. Chinnala, J. Aukunuru, Development of a novel 3-month drug releasing risperidone microspheres, J. Pharm. BioAllied Sci. 7 (2015) 37.

[22] A. Navitha, S. Jogala, C. Krishnamohan, J. Aukunuru, Development of novel risperidone implants using blends of polycaprolactones and in vitro in vivo correlation studies, J. Adv. Pharm. Technol. Res. 5 (2014) 84.

[23] H.O. Ammar, M.M. Ghorab, A.A. Mahmoud, S.H. Noshi, Formulation of risperidone in floating microparticles to alleviate its extrapyramidal side effects, Futur. J. Pharm. Sci. 2 (2016) 43–59.

[24] M.S. Muthu, M.K. Rawat, A. Mishra, S. Singh, PLGA nanoparticle formulations of risperidone: preparation and neuropharmacological evaluation, Nanomed. Nanotechnol. Biol. Med. 5 (2009) 323–333.

[25] A. Khames, Investigation of the effect of solubility increase at the main absorption site on bioavailability of BCS class II drug (risperidone) using liquisolid technique, Drug Deliv. 24 (2017) 328–338.

[26] M.M. Al Omari, M.I. El-Barghouthi, M.B. Zughul, J.E.D. Davies, A.A. Badwan, The role of drug hydrophobicity in β-cyclodextrin complexes, J. Mol. Liq. 155 (2010) 103–108.

[27] M.I. El-Barghouthi, N.A. Masoud, J.K. Al-Kafawein, M.B. Zughul, A.A. Badwan, Host–guest interactions of risperidone with natural and modified cyclodextrins: phase solubility, thermodynamics and molecular modeling studies, J. Inclusion Phenom. Macrocycl. Chem. 53 (2005) 15–22.

[28] M. Jug, I. Kos, M. Bećirević-Laćan, The pH-dependent complexation between risperidone and hydroxypropyl-β-cyclodextrin, J. Inclusion Phenom. Macrocycl. Chem. 64 (2009) 163–171.

[29] M. Jug, M. Becirevic-Lacan, Screening of mucoadhesive microparticles containing hydroxypropyl-beta-cyclodextrin for the nasal delivery of risperidone, Comb. Chem. High Throughput Screen. 10 (2007) 358–367.

[30] D. Shukla, S. Chakraborty, S. Singh, B. Mishra, Preparation and in-vitro characterization of Risperidone-cyclodextrin inclusion complexes as a potential injectable product, DARU J. Pharm. Sci. 17 (2015) 226–235.

[31] A. Celebioglu, T. Uyar, Electrospinning of nanofibers from non-polymeric systems: polymer-free nanofibers from cyclodextrin derivatives, Nanoscale 4 (2012) 621–631.

[32] S. Gould, R.C. Scott, 2-Hydroxypropyl-β-cyclodextrin (HP-β-CD): a toxicology review, Food Chem. Toxicol. 43 (2005) 1451–1459.

[33] A. Celebioglu, T. Uyar, Metronidazole/Hydroxypropyl-β-Cyclodextrin inclusion complex nanofibrous webs as fast-dissolving oral drug delivery system, Int. J. Pharm. 572 (2019) 118828.

[34] E. Hsiung, A. Celebioglu, M.E. Kilic, E. Durgun, T. Uyar, Ondansetron/Cyclodextrin inclusion complex nanofibrous webs for potential orally fast-disintegrating antiemetic drug delivery, Int. J. Pharm. 623 (2022) 121921.

[35] A. Celebioglu, T. Uyar, Electrospun formulation of acyclovir/cyclodextrin nanofibers for fast-dissolving antiviral drug delivery, Mater. Sci. Eng. C 118 (2021) 111514.

[36] A. Celebioglu, N. Wang, M.E. Kilic, E. Durgun, T. Uyar, Orally fast disintegrating cyclodextrin/prednisolone inclusion-complex nanofibrous webs for potential steroid medications, Mol. Pharm. 18 (2021) 4486–4500.

[37] S. Patil, A. Celebioglu, T. Uyar, Orally fast-dissolving drug delivery systems for pediatrics: nanofibrous oral strips from isoniazid/cyclodextrin inclusion complexes, J. Drug Deliv. Sci. Technol. 85 (2023) 104584.

[38] S. Chen, J. Zhou, B. Fang, Y. Ying, D. Yu, H. He, Three EHDA processes from a detachable spinneret for fabricating drug fast dissolution composites, Macromol. Mater. Eng. (2023) 2300361.

[39] Y. Turanlı, M. Birer, Y.T. Birer, R. Uyar, B.Y. Dikmen, F. Acartürk, Oral fast-dissolving risperidone loaded electrospun nanofiber drug delivery systems for antipsychotic therapy, J. Drug Deliv. Sci. Technol. 92 (2024) 105262.

[40] R. Abdulhussain, A. Adebisi, B.R. Conway, K. Asare-Addo, Electrospun nanofibers: exploring process parameters, polymer selection, and recent applications in pharmaceuticals and drug delivery, J. Drug Deliv. Sci. Technol. (2023) 105156.

[41] T. Higuchi, K.A. Connors, Phase solubility diagram, Adv. Anal. Chem. Instrum. 4 (1965) 117–212.

[42] Y. Bi, H. Sunada, Y. Yonezawa, K. Danjo, A. Otsuka, K. Iida, Preparation and evaluation of a compressed tablet rapidly disintegrating in the oral cavity, Chem. Pharm. Bull. 44 (1996) 2121–2127.

[43] M. Haouas, C. Falaise, N. Leclerc, S. Floquet, E. Cadot, NMR spectroscopy to study cyclodextrin-based host-guest assemblies with polynuclear clusters, Dalton Trans 52 (2023) 13467–13481.

[44] H.-J. Schneider, F. Hacket, V. Rudiger, H. Ikeda, NMR studies of cyclodextrins and cyclodextrin complexes, Chem. Rev. 98 (1998) 1755–1785.

[45] J. Xue, T. Wu, Y. Dai, Y. Xia, Electrospinning and electrospun nanofibers: methods, materials, and applications, Chem. Rev. 119 (2019) 5298–5415.

[46] G. Narayanan, R. Boy, B.S. Gupta, A.E. Tonelli, Analytical techniques for characterizing cyclodextrins and their inclusion complexes with large and small molecular weight guest molecules, Polym. Test. 62 (2017) 402–439.

[47] C. Yuan, B. Liu, H. Liu, Characterization of hydroxypropyl-β-cyclodextrins with different substitution patterns via FTIR, GC–MS, and TG–DTA, Carbohydr. Polym. 118 (2015) 36–40.

[48] R. Rukmangathen, I.M. Yallamalli, P.R. Yalavarthi, Formulation and biopharmaceutical evaluation of risperidone-loaded chitosan nanoparticles for intranasal delivery, Drug Dev. Ind. Pharm. 45 (2019) 1342–1350.

[49] A. Nair, D. Khunt, M. Misra, Application of quality by design for optimization of spray drying process used in drying of Risperidone nanosuspension, Powder Technol. 342 (2019) 156–165.

[50] S. Daadoue, M. Al-Remawi, L. Al-Mawla, N. Idkaidek, R.M. Khalid, F. Al-Akayleh, Deep eutectic liquid as transdermal delivery vehicle of Risperidone, J. Mol. Liq. 345 (2022) 117347.

[51] P. Mura, Analytical techniques for characterization of cyclodextrin complexes in the solid state: a review, J. Pharm. Biomed. Anal. 113 (2015) 226–238.

[52] C. Danel, N. Azaroual, A. Brunel, D. Lannoy, G. Vermeersch, P. Odou, C. Vaccher, Study of the complexation of risperidone and 9-hydroxyrisperidone with cyclodextrin hosts using affinity capillary electrophoresis and 1H NMR spectroscopy, J. Chromatogr., A 1215 (2008) 185–193.

[53] Risperidone Dosage, (n.d.). https://www.nhs.uk/medicines/risperidone/.

[54] N.A. Peppas, B. Narasimhan, Mathematical models in drug delivery: how modeling has shaped the way we design new drug delivery systems, J. Contr. Release 190 (2014) 75–81.